Ion beam source for soft-landing deposition

J. P. Biesecker[a] and G. B. Ellison[b]
Department of Chemistry and Biochemistry, University of Colorado, Boulder, Colorado 80309

H. Wang,[c] M. J. Iedema, A. A. Tsekouras, and J. P. Cowin[b]
Environmental Molecular Sciences Laboratory, Pacific Northwest National Laboratory, Box 999, Richland, Washington 99352

(Received 18 June 1997; accepted for publication 20 November 1997)

''Soft-landing'' deposition of molecular ions on various surfaces is important in making exotic radicals, modeling electrochemical double layers, and studying aqueous ion interactions. We have built a new mass-selected ion beam source for soft-landing deposition, designed to produce either positive or negative ions, including ions that depend on ion-neutral reactions (e.g., H_3O^+ and NH_4^+). The ionizer is a free jet crossed by an electron beam, producing a wide variety of positive and negative ions. The simple, short-length, planar ion deceleration minimizes defocusing and space charge effects. It currently delivers mass-selected ions with energies down to about 1 eV and currents of about 10 nA. The design allows easy maintenance. The performance of the ion beam compares favorably with previous low-energy positive ion systems. © *1998 American Institute of Physics.* [S0034-6748(98)03202-X]

I. INTRODUCTION

This article describes a very low-energy ion source, which is able to provide a wide variety of ions, including molecular ions (positive or negative), mass-selected, at nA currents. A source of the pure radicals would be very helpful to unravel surface chemical mechanisms. An ion beam can be used, if after deposition onto a surface they can be neutralized, either spontaneously on a conductor surface, via photodetachment, or by using an electron beam. Many radical species can be made in their mass-selected positive or negative ion forms. Negative ions can be superior to positive ions as the former often neutralize to the ground state, while positive ions will often neutralize to excited electronic states.[1]

Environmental clean-up efforts at many sites require a thorough understanding of ionic reactions, at water-mineral interfaces, in separations or analytical chemistry, or in materials chemistry (as for long-term storage of dangerous wastes). At PNNL[2] and elsewhere,[3] novel experiments for modeling aqueous interfaces are being performed using thin-film ices. A versatile low-energy ion source would permit flexible exploration of ionic processes via such experiments.

There have been extensive efforts to model the electrochemical double layer in vacuum.[3] Vacuum experiments offer more control on the adlayer, and more probes to study the properties of and processes in the adlayer. However, most studies involving ions have been only able to put ions into near-equilibrium states, limiting the kinetic information that can be obtained. And the ions studied have been typically those few that spontaneously form at the surface from conveniently-dosed neutral parents, such as alkali ions, hydronium, or halide ions. It is expected that with a soft-landing ion beam, one can provide a wider array of ions, put them in situations far from equilibrium so as to clearly observe critical kinetics, and even ''sculpt'' the z-dependent ion profiles that constitute the electrochemical double layer or are important in redox couples.

Hyperthermal reactions are those that involve ionic or neutral species, with kinetic energies from 1 to a few hundred eV.[1,4] They are important in plasma reactions at interfaces, and in ion-assisted thin-film materials fabrications.[5,6] They are also important for thermally driven processes that depend on high velocities at the Boltzmann distribution tail. Nuclear waste issues involve hyperthermal processes, as they are central to radiolytic chemistry. Another application is as a probe of surface reaction mechanisms: It is easy to change the ion beam energy to probe reaction barriers.

Electron transfers are important in many of the applications above, as well as for electronics and life processes. An ion source provides an excellent way to apply biases to model thin-film systems to explore electron transfers. These applications help us determine what the ion source needs to do.

Ion impacts at around 10 eV or up often have a high probability of inducing dissociation of the ion or target. Often this must be minimized, via an ion beam energy near 1 eV. To study hyperthermal chemistry, the energy should be conveniently adjustable upward to a few hundred eV.

Studies of radicals or surface ion reactions using surface spectroscopic probes such as vibrational spectroscopy via Fourier-transform infrared (FTIR) or electron energy loss require a minimum of 10% of a monolayer over an area of about 0.1 cm^2. Similar surface coverage is desired for temperature programmed reaction studies (though less can still

[a]Present address: Quantum Peripherals Colorado, Inc., 2270 S 88th St., Louisville, CO 80028-8188.
[b]Authors to whom all correspondence should be addressed.
[c]Present address: Seagate Technology, 7801 Computer Avenue S., Bloomington, MN 55435.

work[1]). A target number offering greater convenience is dosing a full 1 cm^2 crystal. Experiments on ion diffusion or electron transfer[7] which measure the field produced by the deposited ions (via a Kelvin contact potential probe) require typically an order of magnitude less ions. Assuming 10% coverage is 10^{14} cm^{-2} ions, one needs to deposit about 16 μC. A 16 nA beam can do this in 1000 s if the ion sticking probability is unity. On heavy bare metal substrates this probability can be an order of magnitude less,[1] but for deposition on top of water films (or on ''cushion layers,'' see below) unity is likely. A thousand seconds is a good upper limit for the deposition time for convenient experiments. Thus is needed 16 nA beams or more, at the low energy of 1 eV or so.

It is desired that the basic source design can produce a wide variety of *polyatomic* ions, such as H_3O^+, OH^-, NH_4^+, NO_3^-, of both positive and negative sign. In the future it should be able to work with a second beam line, to simultaneously deposit positive and negative ions.

It is critical that the ions be mass selected. Assuming one uses ion ''recipes'' that do not produce more than one species within 1 amu of each other, a resolution of about 0.5 amu should suffice, and a mass range of at least 100 is needed. (Prehydrated ions would demand a higher-yet range.) It would be valuable to be able to check with a second mass spectrometer that this purity is really being achieved.

The beam should be uniform across the area deposited, or other methods (like scanning) employed to make it uniform. The beam intensity should not drift too much. The energy spread of the beam needs to be at most a few eV, otherwise, deceleration of it to 1 eV will not be possible.

Deposition times of 1000 s will require that the sample pressure environment be 10^{-10} Torr or below. Very important is for the ion beam itself not be a source of contamination to the sample.

The number and quality of experiments that actually get done is a strong function of the ease of use of the system. Thus the source cleaning or adjusting should be needed infrequently and be done in minutes. Trying out alternative ion optics should be simple, as should be switching from negative to positive ions. It must be easy to check the beam profile quality and current, even while adjusting knobs, and under the actual deceleration conditions.

During the actual beam deposition, it would be good to know the current, the integrated charge, and any change in the surface potential. The latter is crucial as charging will change the impact energy, and this must be compensated for during deposition. Also related to controlling deposition for many planned experiments is target temperature control. Ions can react or diffuse at very low temperatures. Additionally ''cushion layers'' of inert gases may be important to build. Ten monolayers of argon or methane on top of the actual surface to be studied could help to prevent damage from the incoming beam. For example, a nitrate ion hitting an argon surface will have limited options to produce chemistry associated with the impact energy, compared to hitting a water surface or bare Pt. Also, as the energy of solvation at a water interface can be 3 eV and up, a cushion layer can be useful: If the ion hits the inert cushion layer, the immediate solvation energy release will be less (1–2 eV), and there will be less options for it to induce chemistry. When the ion later encounters the water, the solvation energy release will only be the incremental amount. After deposition, the target can be warmed just enough to remove the cushion layer (or permit the ions to diffuse through it). Ideally, control from 25 K and up during deposition is desirable.

Ion beams have been made for a century, however, no existing commercial or laboratory sources meet all of our needs, though some compare favorably with ours in some regards. They will be mentioned prominently in the design discussions below, and some comparisons of this new source to these will be made. Special thanks in the Acknowledgment section are made to several researchers for sharing their insight via discussions.

This source built meets the goals set, having been shown to date to be able to deliver up to 45 nA of mass-selected positive molecular ions at an energy of 3 eV, 10 nA, or more at 1 eV, and several nanoamps of Cs^+ at 0.7 eV.[8] Up to 20 nA of ions formed from ion-neutral reactions, like H_3O^+ and NH_4^+ have also been made. It is configured to produce molecular negative ions with the addition of a magnetic deflector to reject electrons, but this capability has not yet been demonstrated here (similar sources have been shown elsewhere to be good at this). Details of the machine and operating methods, particularly crucial to maximizing its performance in soft-landing ions are discussed later in the context of two example experiments.

II. ION BEAM DEPOSITION SYSTEM DESIGN

A. Overview

The design is shown in Fig. 1. There are five regions in the ion source: the ionizer region, the collimation region, the mass filter region, the drift region, and the deceleration region. A sixth region, the target chamber, is the ultrahigh vacuum (UHV) system to which the ion source is coupled. The ions are prepared in the ionizer region, extracted and formed into a beam in the collimation region, mass selected by a Wien filter and decelerated in the last 1 cm of their trip to the 1 cm diameter sample in the UHV chamber. All the sections are separated from each other by 1 cm diameter apertures or tubes. The ion energy to ground is defined by the bias potential applied to the ionizer region, the ions typically traversing most of the source at 300–400 eV. The ions are decelerated by biasing the sample to a potential close to that of the source region.

B. Ionizer

Our general purpose ionizer is a ''high-pressure'' nozzle ionizer, where electrons or ions initially produced can encounter neutral species. When an electron beam or electrons in a plasma (or discharge) ionizer hit molecules at 10–200 eV, they tend primarily to form positive ions, the familiar ''cracking pattern'' of the parent species seen in mass spectrometry. If the local gas density is high so that before leaving the ionizer region, the primary ions undergo collisions

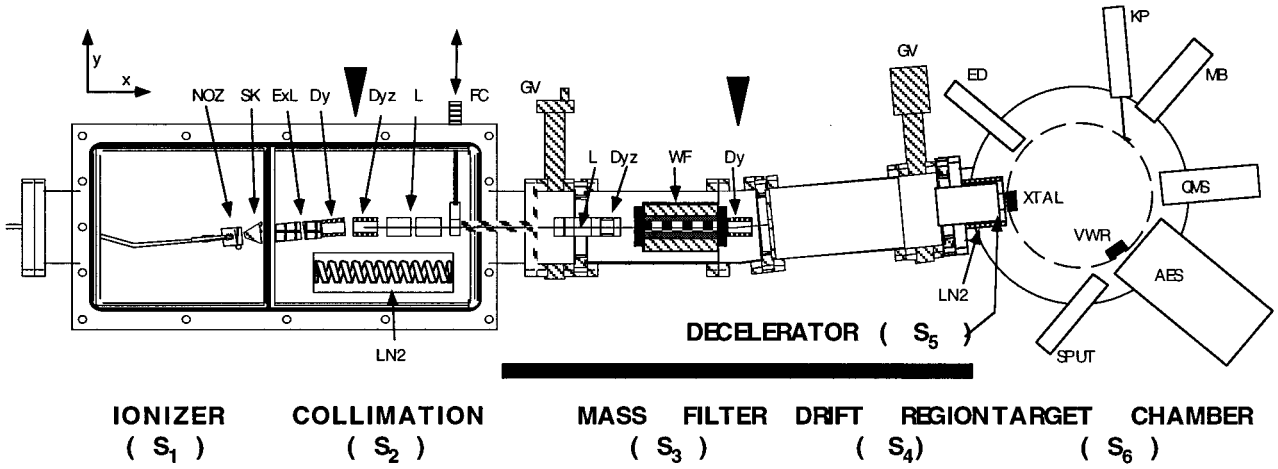

FIG. 1. Ion beam system. In the simplified top-view scale drawing of the ion source, the tagged items are: NOZ=nozzle beam ionizer, SK=skimmer, ExL=extractor/lenses, Dyz=*y* and *z* deflectors, Dy=*y* deflector, L=lens, LN2=liquid nitrogen cooled cryopanel or shroud, FC=Faraday cup, GV=gatevalve, WF=Wien velocity (mass) filter, XTAL=crystal target on its holder, ED=effusive doser, KP=Kelvin probe, MB=molecular beam, QMS=quadrupole mass spectrometer, AES=Auger electron spectrometer, SPUT=ion sputter gun, VWR=ion beam viewer. Pumps are for S_1 through S_6: 5300 ℓ/s diffusion, 805 ℓ/s diffusion+7000 ℓ/s cryopanel, 240 ℓ/s turbo, 240 ℓ/s turbo, cryoshroud with Ti sublimation, 400 ℓ/s ion+about4000 ℓ/s cryopumping. The wedge symbols indicate where the two 5° bends take place. The black bar is 1 m scale.

with neutral species, then new classes of ions are possible. For example, H_2O^+ ions formed by electron impact have a near barrier-less reaction with H_2O molecules in the gas phase to form H_3O^+ and OH.[9] NH_4^+ or hydrated ions can also be formed this way. Most plasma ionizers have a high concentration of low-energy electrons which can readily attach to many molecules to form negative ions. Electron impact sources create similar low-energy secondary electrons, as high-energy primary electrons knock other electrons out of molecules. The negative ions produced can also undergo further ion-neutral reactions.

Several high-pressure plasma sources are in widespread use. However, most are unsuited to our task for the following reasons: They tend to have too high an energy spread, so that deceleration would not be possible, and the plasma conditions are often too ''aggressive,'' tending to produce highly dissociated or only very stable ions, and ions with very high internal temperatures. The typical intensity is too small (1 nA), and they often require frequent cleaning and filament replacement. The Freeman source and its variants[10,11] are based on a hot filament encased in a can with a small hole in it, at around 1 Torr, biased so as to produce a plasma. A Brancomb source[12] uses an enclosed discharge with built-in magnetics to suppress electrons when used for negative ion production, and can usefully produce many ions such as 10 nA of mass-selected OH^-.[13]

Our ionizer is an expanding supersonic jet of gas crossed by an electron beam from a nearby filament. It is patterned (in general, though not in many construction details) most closely after one currently used by Lineberger and co-workers.[14] The ion source depicted in Fig. 2 consists of a nozzle, an electron source, a skimmer, and a mesh-walled containment region in which the ions are born. The nozzle is a 1/4 inch male Cajon VCO blank-off cap fitting, with a 1 mm diameter (by 2 mm long) aperture. It is electrically isolated via a ceramic tube break, so its voltage can be optimized. The expanding beam is intercepted by the skimmer with a 1 cm diameter hole and is extracted by lenses in the extraction region.

The filament is a W wire coil, from an automobile headlight. It is located just outside the mesh region defining the ionizer potential, and should give a crudely collimated ribbon beam of electrons. The filament holder was mounted independently on the optical rail, and varied in distance from 0.5 to 2 cm from the skimmer. The filament was run at 10–30 mA of emission current. There is a repelling plate behind the filament which can be biased from −16 to −300 V with respect to the ionizer. The electron energies have been about 100 eV. The nozzle was 2–4 cm away from the skimmer. Nozzle pressure was typically between 2 and 4 Torr. The ion energy is determined by the voltage of the cage around the ionizer, and has typically been run 300–400 V above ground. It was decided to keep the flight path at ground, and float the ionizer (and target for deceleration) rather than float the flight path and keep the other two near ground.

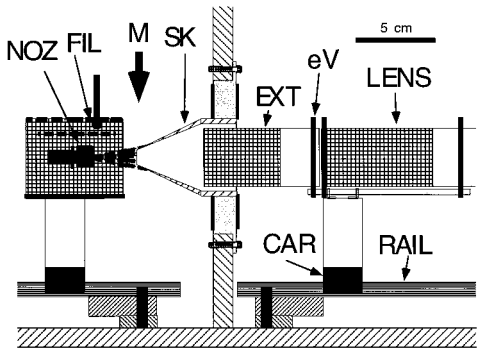

FIG. 2. Nozzle/extraction region. Nozzle region components are: NOZ=Nozzle; FIL=filament; M=location for optional electron rejecting magnetics; SKI=skimmer (1 cm aperture); EXT=mesh extractor lens; eV=Kimball Physics 2 inch ''eV Part'' plate; LENS=ion lens; RAIL=Newport mini-optical rail; CAR=optical rail carrier.

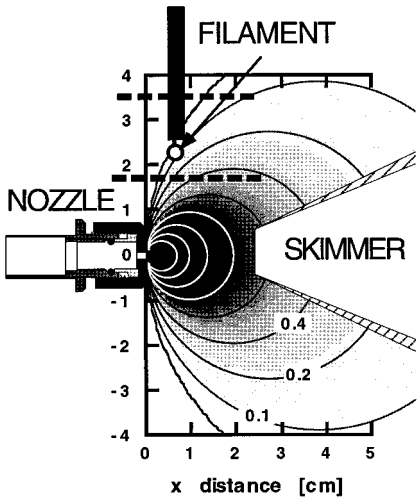

FIG. 3. Free-jet and collisions. The nozzle region is shown with the calculated molecular beam density, expressed as collisions/cm (approximately) experienced by ions, neutrals and electrons. Contours are spaced by factors of 2. Shading is in proportion to density too.

With a nozzle diameter of 1 mm, and 2–4 Torr stagnation pressure, many collisions occur in the expanding gas before it thins. Shown in Fig. 3 is an approximate density of the intensity in front of the nozzle. It is calculated by assuming the outgoing fluence has a cosine-squared dependence on angle (typical for supersonic expansion), and that the density falls simply as

$$\rho(x,y)=\cos^2(\theta)r_0 d_0^2/(d_0^2+x^2), \tag{1}$$

accurate beyond several nozzle diameters away from the nozzle.[13] Here x is along the beam axis, d_0 is the nozzle diameter (1 mm here), and $y/x=\tan(\theta)$. Further, to give some feel for the effect of collisions, the density is expressed as $g=$collision/cm that would roughly be experienced assuming air-like collision mean free paths:

$$g(x,y)=\rho(x,y)/(0.001\ \text{Torr}\times 5\ \text{cm}). \tag{2}$$

The collision/cm traveled will be somewhat different for ions, neutrals, and electrons, being typically somewhat larger for neutrals than that for the ions and less than that for the electrons. The skimmer is far enough away that collisions have largely ceased before reaching it. But the ions created near the electron beam will suffer some collisions before getting out, depending on where the filament is positioned. One concern is that the electron beam may have trouble penetrating the neutral cloud, to uniformly ionize the neutral beam. It helps to run the electrons at an energy where the electron penetration is adequate, and to adjust the filament position carefully, which is done by several manual adjustments. Soon the filament will be mounted on a linear translator so it can be adjusted from outside.

The source was only briefly (to date) tried for making negative ions,[14] but did not immediately succeed, as too many electrons were being extracted. Almost all negative ion sources have an electron-suppressing magnetic field.[12,15,16] In the future an electron suppressor will be inserted near where Fig. 2 indicates.

C. Extraction/collimation/deflection

The collimation region consists of a 1.5 in. diameter cylindrical stainless mesh extraction cylinder, and a series of three additional cylindrical focusing lenses and deflectors. The extraction and focusing lenses are constructed from stainless-steel Kimball Physics ''eV Parts.'' The extraction lens was from 10 to 300 V more negative than the containment region, to extract the positive ions from the source region. The ions exit through a 1 cm aperture into the mass filter region. The extraction lens and first deflectors are made of mesh to allow the neutral beam flux to dissipate (otherwise the local pressure inside of these lenses would be sufficient to seriously attenuate the ion beam).

The skimmer orifice was designed very large (1 cm) based on the experience with the University of Colorado beam source;[14] they had found that as they increased their skimmer size up to 1 cm, the ion current they could successfully produce increased strongly. The rest of the interchamber apertures are also 1 cm, so that the beam would not have to be focused tightly at any point. This would minimize the aberrations to the beam, which could later prevent efficient deceleration. This causes special differential pumping concerns discussed later. Two xy deflectors in this region align the beam, and give it a 5° bend, to separate the ions from the intense direct neutral flux beam coming from the nozzle.

D. Mass selection

Several options for mass filtering were considered. A quadrupole was rejected as the exiting flux tends to be rather diffuse, and not well suited for manipulation or deceleration afterwards. A 90° sector magnet would be a good choice, though in the lab where this was first installed, this would have caused serious space problems. Adequate resolution was possible (see below) with a 6-inch Wien filter (Colutron 600-H Wien filter[11]), which also has the advantage that it is a straight-through device. By turning it off the total ion current through the system can be used. It is a velocity filter with static crossed magnetic and electric fields. The filter magnet coil is capable of running at 500 W. The coils are cooled by R-134a refrigerant whenever the magnet power is on. Since all the ions were born with the same energy, their different masses cause their velocities to be different. A 45 cm drift region follows the Wien filter to provide better mass resolution. The drift region ends with a 1 cm by 1 cm selection slit.

E. Deceleration and space charge issues

Deceleration is a crucial process for this source. Space charge must be dealt with carefully for this to occur successfully. We also discuss space charge ''blooming'' of the beam in this section.

The beam will spread transversely (''bloom'') due to space charge creating a radial field in the beam. The lower the beam energy, the higher the charge density and the more space charge will cause beam divergences. For a uniform flux, cylindrical, initially collimated beam of diameter d_0,

translational energy KE (in eV), and mass m, the current that will cause the beam to increase about twofold its initial diameter over a flight path of L, is[17]

$$I = 1 \times 10^{-6} \text{ amps}(\text{KE/eV})^{3/2}/(\text{m/amu})^{1/2}(d/L)^2. \quad (3)$$

The current will be less for larger masses. For a 100 amu beam at 16 nA with $L = 45$ cm (the drift region flight path), one gets

$$\text{KE} = 47 \text{ eV}(\text{cm}/d)^{4/3}. \quad (4)$$

For $d = 1$ cm, this is 47 eV, and for 0.2 cm, this is 400 eV. At $I = 100$ nA the two beam energies are 150 and 1300 eV. A 1 cm beam size will cause less problems with space charge induced spreading, and give some options of approaching 100 nA of beam currents without having to increase the beam energy beyond that which is convenient and easier to decelerate.

When the ion beam is decelerated, the space charge spreading of the beam must be avoided. A 1 eV beam across 10 cm, for mass 100 amu, Eq. (3) would be limited to 10 nA for a 1 cm beam, and 0.4 nA for a 0.2 cm beam. The key to bright deceleration is to keep the distances short over which the ions will travel at low energy. This was the conclusion of Rabalais and co-workers,[5] for example, when they found that by abandoning an elaborate and long decelerator by shorting together 34 out of 37 plates, they could get much higher currents at low energy.

The above results point us toward a very short decelerator with about a 1 cm beam size. Our design for the deceleration optics then is to employ a flat field over a very short distance of about 1 cm. For a wide beam decelerating, one should consider the space charge potential in the axial direction, not just the radial direction covered by Eq. (3). An infinitely wide planar decelerator will have a limiting current (per 1 cm area) given by the Child's Law formula (used for electron emission)[17] of

$$I = 5.4 \times 10^{-8} \text{ A cm}^{-2}(\text{KE/eV})^{3/2}/(\text{m/amu})^{1/2}(L/\text{cm})^2, \quad (5)$$

where KE is the initial beam energy. For $L = 1$ cm, $K_E = 400$ eV, a 1 cm^2 beam area, and a mass of 100 amu, this gives $I = 43$ μA! Thus this system should have little problem with axial space charge effects.

As shown in Fig. 4, the deceleration region consists of a collimation lens, a 0.12 cm thick stainless plate with a 1.2 cm aperture covered on each side by an electroformed, 300 lines per inch, 78% transmitting nickel mesh, and a front flat with another 1.2 cm aperture, slightly larger than the sample diameter. Under our current run condition, the meshed plate is at ground while the front plate and the sample are biased together (nearly together, as discussed later) to a positive potential. The sample is brought into the hole of the front plate to form part of a nearly planar electrode and the ions are slowed down by the planar field created between the two plates. A grounded structural aperture between the double mesh and the sample was shielded by a plate and cylinder, and was to be biased in principle about 1/2 way between the

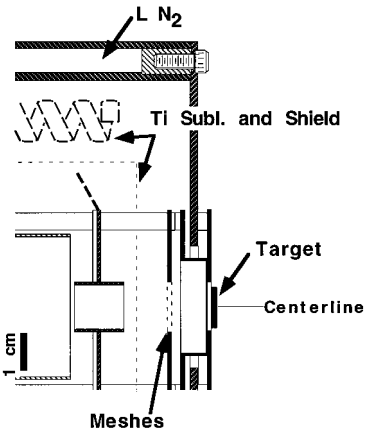

FIG. 4. Decelerator details. The decelerator region is shown, with the target (whose holder is not shown) moved up against final decelerator plate.

mesh and target voltage. The geometry shown in Fig. 4 is not in the decelerator region as planar as desired, but it seems to work adequately.

Vestel *et al.* decelerate 1 nA beams down to about 0.5 eV, using a well-documented exponential field decelerator, and are space charge limited at this current for their geometry.[18] Strongin and co-workers[19] have a short decelerator in some ways similar to ours (see the performance section). They get considerably increased currents to the sample at very low energy (100 nA at 1 eV) by putting a strong axial magnetic field in the deceleration region. They use a permanent disk magnet placed behind the sample. We did not choose this approach, as the magnetic field would also permit ion energies of up to 5 eV perpendicular to the field to hit the sample while it was biased to allow only 1 eV perpendicular to the surface.

A single mesh (or coarser meshes) would not give nearly as flat a field due to field penetration through the meshes. The calculated field (MacSimion) is plotted in Fig. 5 for two situations: sample at the hole, and sample 1 cm away from the hole. For either case, there is negligible field penetration in the region before the meshed plate. When the sample is in the hole, the calculated field is indeed flat and trajectory simulation show little change in collimation or beam uniformity. However, when the sample is away from the front plate, the field in this region is not flat and a divergent lens is created. The ion trajectory simulation also shows deflection of ions not traveling along the center line. The difference between the two situations is clearly seen in our deceleration experiments, as will be discussed in the performance section. Note that one should be concerned about the meshes making a shadow on the sample. This would give nonuniform ion dosing. However, our use of a very fine pitch mesh (and care to limit the moire pattern between the two meshes by rotating the second one) means that casting a shadow would require a better collimated beam than our geometry requires, or than our measurements have ever indicated. Also, the very slight lensing effect that the field penetration makes each grid square have helps to diffuse the grid shadow. One could slightly scan the sample during dosing to prevent any possi-

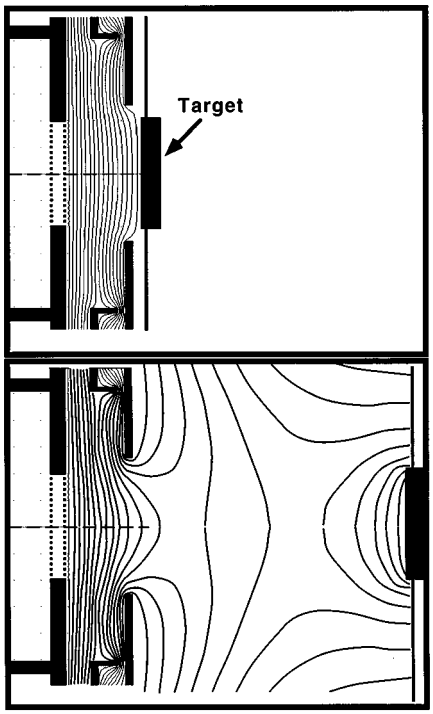

FIG. 5. Calculated fields in decelerator region. The fields and some trajectories for a 400 eV beam decelerated down to 1 eV are calculated with sample nearly in the proper location (top), and 4 cm further back (bottom).

bility of having grid shadow effects, but we have yet to see evidence that this is a problem.

F. Differential pumping

Having 1 cm apertures, and the occasional need to dose for 20 min or longer without significant contamination problems, makes differential pumping both crucial and challenging. A recent study we did (discussed later in this article) described temperature programmed desorption (TPD) experiments of ion-derived species at the 0.001 to 0.01 monolayer regime after just such long ion doses, which required condensible or reactive gas backgrounds, including parent species from the ion source nozzle, to be as low as 10^{-12} Torr. It is most crucial that the ion beam be stripped of the large neutral flux. This is accomplished by deflecting the beam 5° in the collimation region of the source. A 5° bend was chosen instead of a 90° bend, to minimize aberrations of the beam caused by excessive handling. Also, this kept our beam line more straight, which for our lab was an advantage. Note that two deflectors in series accomplish this bend. This is because not only must the the final angle be correct, but also the beam must be spatially centered on the new beam axis. Alternatively, one could use a single deflector that was movable, or simply use an asymmetric deflector, where the attractive and repulsive plates had independently controlled voltages.

The large apertures also create not only more gas load effusing between chambers, but shift the importance of ''direct beaming'' over simple effusion. Without the 5° bend, the direct beam from the nozzle being even slightly clipped by down-beam apertures would become the dominant gas load in each chamber following, instead of chamber-by-chamber intereffusion. Even with a 5° bend in the collimation region, the collimation chamber exit aperture acts as a substantial effusive beam, whose flux would be too high at the target (as this is not differentially pumpable). It would also be the dominant load for the last differential chamber. It was crucial to add a second 5° bend. This was added at the junction of the mass filter and drift regions.

TABLE I. Delta pressures of ion source region with D_2O beam.

Region	Delta pressure
Nozzle	2.6 Torr
Ionizer	2×10^{-5}
Collimator	2×10^{-7}
Wien	6×10^{-8}
Drift	1×10^{-9}
Target chamber	$<1\times10^{-11}$

To further enhance the differential pumping, the 1 cm aperture between the collimation and mass filter regions is a tube about 10 cm long. In the future tubes should replace two of the other flat chamber apertures. In the collimation region a liquid nitrogen cooled cryopanel is used, and was essential to maintaining low enough backgrounds during our TPD studies with the ion source.

The sample is pressed up against the decelerator during deposition. This last region can help us reduce background pressures locally, even though it is not strongly isolated from the target chamber. Surrounding the deceleration electrodes is a liquid nitrogen cooled shroud, which for our most demanding TPD experiments was crucial. Room was left inside of the shroud to add a titanium sublimation filament, and a shield to protect the ion optics from direct titanium deposition. This (if used) would provide additional local pumping speed, and would also allow, via radiative heating, a quick bakeout of the deceleration optics.

As shown in Fig. 1, starting from the ionizer going to the target chamber, there are six separate pumping regions. The mass filter and drift regions are baked with heating tapes to reduce their outgassing. The drift region ultimate pressure is about 1×10^{-9} Torr. The changes in pressure when a water ion beam is running is given in various regions in Table I, with the cryoshrouds and panels cooled with liquid nitrogen.

G. Electronics

The ionizer is powered by a floatable Spectrum Solutions[20] filament supply, whose common is biased with an external supply when higher than a 300 eV beam is used. The current to the skimmer and first few extraction/collimation elements can be microamps, so the Spectrum Solutions high current capability is used to drive these. Most of the rest of the elements and deflectors are driven via a set of resistive voltage dividers that feed off floating $+1000$ and -1000 V power supplies. The deflectors are driven using dual ganged pots over a ±100 V range. The common of the voltage dividers can be floated is tied to the flight path tubes. A polarity switch swaps the $+1000$ and -1000 V power

supplies, to make it easier to change from positive to negative ions.

The ion current is monitored at several points along the ion path. It is convenient to measure ion currents hitting key apertures along the way, but as this represents the ions that are missing the proper path, it is often not productive to tune up the source using these currents. On-line Faraday cups are better, and there is one in the end of the collimation region. A motion feedthrough tilts in an on-edge corrugated foil ion collector (to reduce possibility of losing secondary electrons). When retracted a cylinder shields the ion path from the fields of this collector. The ion beam viewer (see below) actually is more sensitive (even visually) for finding the beam when it is badly mistuned than the electrometer on the sample. For the ions examined (water ions, hydronium, Cs, ammonia, ammonium) there is no evidence of losing charge on the collector due to either ions bouncing still charged, or ejection of secondary electrons. Near the target, electrons are produced by ions hitting the decelerator grids, giving as much as 10% conversion (when ions are fully reflected by the target back to the grids). A 4 mT transverse magnetic field to suppress this will be added.

The sample must be carefully isolated, as it is biased at 300–400 V typically while ion dosing, to allow monitoring the ion current without interference. Our sample is cooled via a closed-cycle helium refrigerator (APD) with a sapphire spacer for electrical insulation. The sapphire must be carefully cleaned. Our crystal heating is done radiatively with nearby W filaments (four more headlight filaments), so it has no direct connection to the heating power supplies. When the target is below room temperature, electron emission from the filaments can be avoided. The insulators for the target are shielded from evaporating *W*. The target is connected to two thermocouple pairs, which are used to control the temperature during the experiment. The thermocouple signal goes directly to a Eurotherm 900 series temperature controller, which can float with the sample. The Eurotherm has fair electrical isolation, is quick enough response to control our small sample, and has excellent stability for use in the cryogenic regime. Its manuals and operation we find awkward. A digital voltmeter with a GPIB computer interface is also connected to provide a second opinion as to the sample temperature, and this unit is interfaced to a data collection program. Typically the leakage currents associated with these devices when the target is biased to 300 V are much less than a nA.

The ions are decelerated by the target potential, which is provided by a separate power supply. This is fed to the sample with a Keithley electrometer placed in series. We added internally to this electrometer an isolation amplifier, so that it could transmit the analog current reading to the computer (at ground potential). The deceleration power supply is controlled by the data collection computer's analog output.

When the deceleration voltage is being scanned, the electrometer gets a capacitive current, needed to charge up the cables to the target and any internal capacitance in the electrometer. At $+1$ V/s, this is about -1 nA for our system. This is a small annoyance, but not much problem.

H. Beam viewer

To uniformly dose the target with ions the beam must be reasonably uniform. While one can move the target around to roughly measure the beam profile, this is tedious, and not easily applicable to when the beam is actually being decelerated. A visual beam viewer was installed. It is rotated in front of the ion doser, then tilted in to put the viewer front flush with the ion source exit aperture. Now the viewer front can decelerate ions just like the target can. The viewer front is a Kimball Physics eV Part with a 3/4 inch hole and a Buckbee-Mears 1000 lines per inch nickel electroformed mesh spot welded to the front. (The mesh is only 0.0001–0.0002 inch thick, which limits the stray magnetic fields the Ni can generate.) Behind it is a 25 mm Galileo channelplate electron multiplier, whose front is typically biased about -700 to -800 V to ground, and the rear grounded. Ions hitting this create electrons which are amplified, and pass out the other side. There they hit an eV Part phosphor screen at about 3000 V. The screen is viewed with a sensitive monochrome television camera, with the monitor adjacent to the ion tuning controls. We measure the current to the view screen front mesh as well.

A single mesh rather than a double mesh was used, to eliminate moire patterns. A 1000 line per inch mesh, 50% nominal transmission (we measure 35%) or finer is required, as otherwise field penetration can be severe. Using MacSimion to estimate the field penetration, with a 400 V/cm field on the front of the view mesh, and a -4000 V/cm field on the rear, the field penetration (for a 1D grid simulation) is 0.6 V.

I. Miscellaneous

Several features add to the convenience of the ion source. First, for easy maintenance, the ion optics were done so that wiring (and alterations) would be easy. Most of the ion optics are mounted on vacuum grade Newport Optics mini rails, to allow easy removal or adjustment. Pads and pins were added during construction on the ionizer/collimation chamber so the rails could be precision placed. Optics mounted inside of the Wien region are also mounted via such rails, mounted off special double-sided Conflats. All wiring for the ionizer and collimator optics come from the side walls. A large aluminum rectangular flange hinged to the chamber opens up these two region for easy access. A typical time scale for changing a broken ionizer filament is about 30 min. Wiring (and cooling fluids, for Wien filter) passes to the optics in the other sections via the specially-made double-sided Conflats (seen in Fig. 1), by way of radial mini-Conflat ports. So this wiring can all be done on the bench, and the completed, aligned sections can be easily inserted into their tube housings. These same double-sided Conflats also mount the apertures (or tubes) that isolate the chambers. These work fairly well, though in future sources we may prefer removable side walls for the later sections. The separate ion chambers have wheeled stands.

The Extrel mass spectrometer that is across the chamber from the ion source is excellent for checking the ion beam composition with and without Wien filter mass selection of

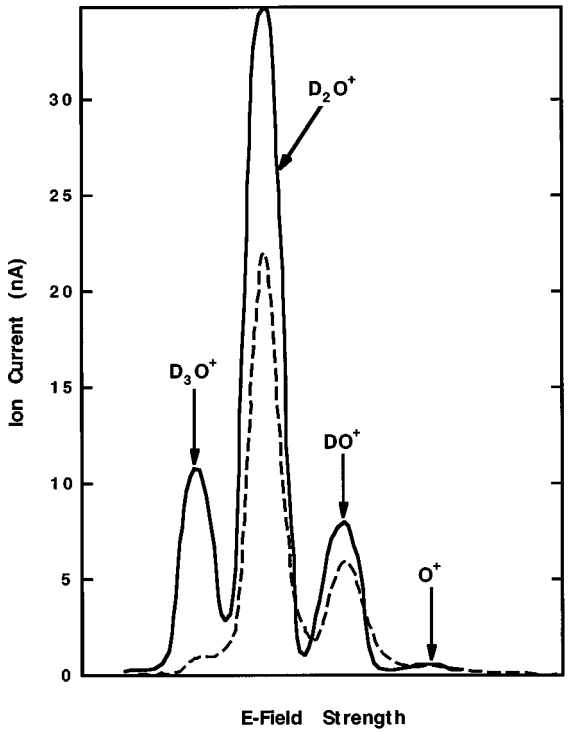

FIG. 6. Ion beam from D_2O feed gas. The mass-analyzed current delivered to the target as a function of the Wien filter electric field, for D_2O feed gas pressures of 2.5 Torr (lower curve) and 4.5 Torr.

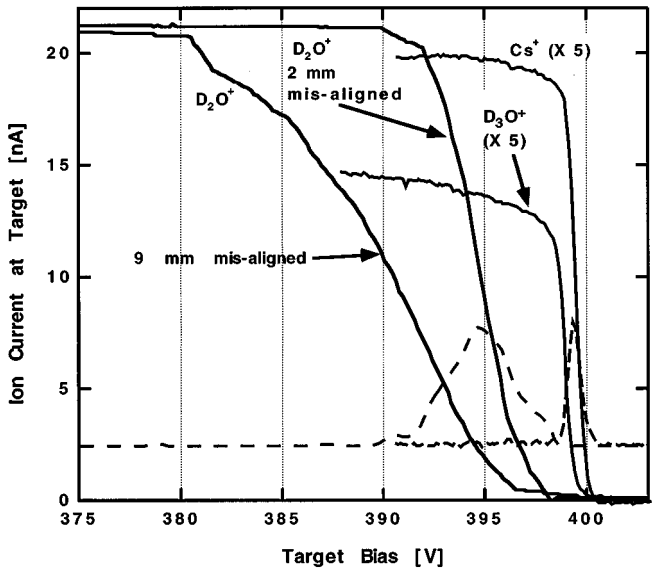

FIG. 7. Stopping curves for ions. Stopping curves for two 20 nA D_2O^+ beams, a 3 nA D_3O^+ beam (from a separate experiment), and a 4 nA Cs^+ beam. One D_2O^+ curve shows the effect of moving the sample significantly away from the ideal position. The derivatives of the narrow D_2O^+ and the Cs^+ curves give the beam energy distributions.

the ion beam. For this the quadrupole rods must be floated close to the ion beam energy. The ion optics in the ionizer, particularly the skimmer, create some severe ion focusing (and perhaps aberrations), which may not be ideal.

A crucial instrument for our experiments is a Kelvin probe, to measure the workfunction changes caused by ions deposited on a surface or ice multilayer. We use a McAllister Kelvin probe for this.[21] It is computer-driven, and fairly sensitive. Our very large swings in work function during our experiments (up to 70 V) required some slightly customized versions of the software package, which they conveniently provided. A dedicated PC runs the Kelvin probe and it outputs an analog version of the measured contact potential difference, which our other computer inputs to our main data collection program.

III. PERFORMANCE

Various properties of the ion beam for feed gases of D_2O and NH_3 will be discussed, as will the results for replacing the ionizer with a small Cs^+ ion dispenser.[8]

A. Ion creation and selection

Four positive ions were created by feeding D_2O into the ion source—O^+, DO^+, D_2O^+, and D_3O^+. The amount of various ions created was measured by the current collected by the sample, as the Wien filter electric field is ramped. This is plotted in Fig. 6 under two different nozzle pressures, 2.5 and 4.5 Torr, for about 30 mA of electron emission. The ion energy at the Wien region is 400 eV. Clearly seen is the four peaks of D_3O^+, D_2O^+, DO^+, and O^+ with 1 amu resolution by running the magnet at only 30% of maximum power. With the Wien filter set at the center of the D_2O^+ ion peak, the mass spectrum with the opposing Extrel shows less than one percent of D_3O^+ and DO^+. Mass one separated peaks, as for H_2O feed gases, have not been quite satisfactorily resolved, perhaps limited by the Wein filter field uniformity. It is clear from both curves in Fig. 6 that ion-neutral collisions are occurring, as this is how D_3O^+ is formed. As expected, the D_3O^+ peak is relatively higher at the higher pressure.

Ammonia was also used as a feed gas. At low pressure a normal cracking pattern distribution was obtained, but with about 3% NH_4^+ evident. At higher nozzle pressures and after adjusting the nozzle/skimmer/filament positions, the NH_4^+ could be made to predominate NH_3^+ by as much as a 3:1 ratio. For some experiments, the normal ionizer was replaced by a Cs^+ ion source[8] in front of the skimmer.

The transmission of the Wien filter can be judged by comparing the total ion current with the Wien filter turned off, to the sum of all the peak ion currents in the mass-resolved spectra. A precise determination of this is made more difficult by the unavoidable readjusting of some of the potentials that are needed when switching to mass-analyzed mode, but the transmission is typically on the order of 75% or higher.

B. Stopping curves

The ion current at the target as the target is biased to progressively more positive potentials is shown in Fig. 7. The ion currents are nearly unchanged until just a few volts below that needed to repel the ion beam, then they drop off to zero over a few volts. The derivative of the stopping curve gives the (apparent) beam width. Initially 3–4 eV wide molecular ion beams were obtained; now more typically the beam stopping curves fall over 1 eV or less. One curve for the 400 eV D_2O^+ ion beam was taken with the sample about

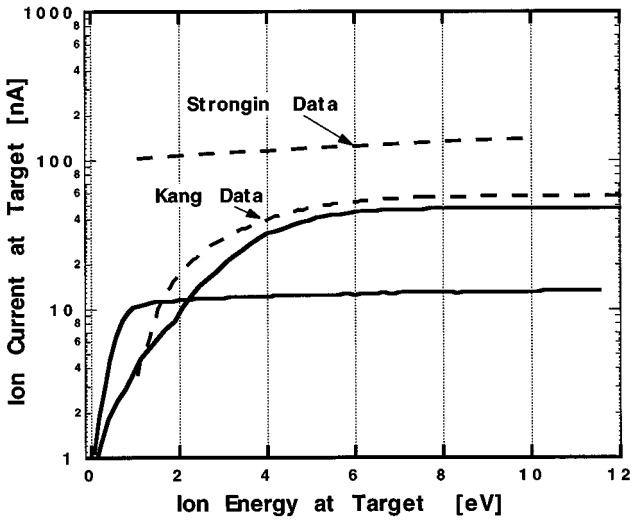

FIG. 8. Comparison of several sources. Stopping curves for various ion beams at low energy: Top curve is from Strongin *et al.* (Ref. 19), the second, dashed curve is from Kang *et al.* (Ref. 15), and the two solid curves are D_2O^+ beams from this study.

2 mm further away than the ideal position (which is flush against the ion beam exit aperture), which only slightly degrades the stopping curve. Indeed, also shown in Fig. 7 is a stopping curve for a Cs^+ beam from the ion dispenser. Published work and the company's specifications say that its energy width is a few times kT at the 1000 °C emitter temperature, that is about 0.3 eV FWHM.[22] The Cs^+ ion beam primary energy in Fig. 7 was 300 eV, and the stopping curve was shifted up 100 V for this figure. The derivative of this stopping curve is 0.75 eV FWHM (0.6–0.8 eV typically) which may represent the resolution of the deceleration process. Our MacSimion calculations indicate that the fundamental resolution of the deceleration is less than 1 V. The FWHM seen for the older water beam data reflects the ion beam kinetic energy spread, due probably to the spread in the extraction field potential over the range of positions where they were created. This is supported by the observation that when the skimmer potential with respect to the rest of the ion creation region in increased, the measured energy spread increased greatly.

How very important it is to control the geometry which shapes the potentials in the decelerator is shown in Fig. 7, where the target has been moved back 9 mm from the ideal position. The stopping curve now is many volts wide, and would for many of our experiments not allow us to deliver enough current at low energy.

Figure 8 shows stopping curves for this source, compared to other ion source designs. The most striking, intense result is that of Strongin *et al.*[19] They utilized the magnetic field of a permanent magnet behind the sample to confine the charged particle motion in deceleration. Their beam passes through an aperture plate with a 7 mm hole, which is covered by a 90% transmitting W mesh, before hitting the sample. The sample is anywhere from 2 to 5 cm from the aperture. The axis of the magnetic field lined up with the sample normal, with the strength of 2000 G on the surface. Their data show an Ar^+ ion current of greater than 100 nA at 1 eV energy with an longitudenal energy spread of less than 0.5 eV, where ion energy is measured as the potential difference between the sample and the source. The magnetic field certainly is an important part of their success. Yet one feature which they describe as a benefit is also a drawback. In that field, an ion could have up to 5 eV of kinetic energy transverse to the magnetic field and still hit the surface. We do not want an unknown amount of transverse energy in the beam. Also important for them is the short distance over which the ions are decelerated, which limits the space charge. For their 2 cm distance, space charge spreading should not be a problem: What the magnetic field is doing is compensating for the lensing effects of the fields near the sample. Rather than use a magnetic field, we chose to keep the fields nearly planar.

Figure 8 shows some ion beam successes of Kang *et al.*,[5] who use no magnetics in the decelerator. Not shown is the result mentioned earlier, of Vestal *et al.*,[18] which got about 1 nA beams down to about 0.5 eV. Both the Kang and the Vestal source have similar long decelerator lens assemblies, but Kang runs theirs so that the deceleration occurs abruptly in the very last section. So they have a much higher current capability as a result of being less affected by space charge limits.

The energy spread of our beam is similar to that of Kang *et al.*, but worse than that of Vestal *et al.* and Strongin *et al.* Both Kang *et al.* and Strongin *et al.* used a Colutron ion source which has an energy spread which can be as low as 0.1–0.3 eV. Vestal *et al.* used a similar ion source. All three groups ionize the gas in a closed cavity by electron bombardment.

Ion sources for materials deposition studies typically need to be much more intense. An example of a such an optimized ion source is that of Bayati *et al.*[23] They produce 3.7 cm^2, 370 μA beams using a Freeman plasma source. Because the energy width is about 7 eV, this source is useful only above 5 eV. Cooks' group has an ion machine for surface studies, which has been used for soft-landing ions on surfaces.[24] Originally limited to about 10 eV and up, in more recent use it has been useful down to 3 eV impact energies.[24]

C. Beam uniformity

Generally the electron-impact/molecular beam ionizer tends to give smoother ion beam profile than does the Cs^+ ion source, the latter giving a somewhat grainy ion pattern, which seems to correspond to a poor, magnified image of an irregularly emitting source. Both were adequate for uniformly illuminating a 1 cm sample. One should take care to orient the double meshes to minimize moire effects. It was easy to illuminate less than all of the sample, as spot sizes to 0.01–0.1 cm^2 were possible, and the beam can be noncircular. With the beam viewer biased to mimic the deceleration conditions, we find that in tuning up the source for maximum current, one usually get uniform illumination provided that one does not overfocus with the last lens just before the decelerator (which is otherwise tempting as it increases the current).

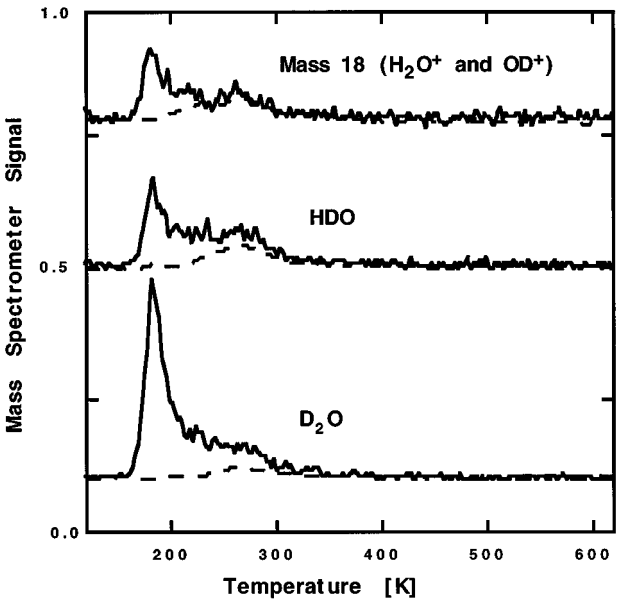

FIG. 9. Background vs ion dose. Temperature programmed desorption from a Pt(111) crystal after dosing for 30 min with the sample biased to reject all ions (dashed curves), and biased to permit them to land (solid curves) at 3 eV, for an 11 nA (at 3 eV) D_2O^+ ion beam. High hydrogen background discussed in text underwent dissociative desorption on Pt followed by exchange with D_2O, yielding anomalously high amounts of desorbed H_2O and HDO.

D. Background during ion deposition

To check the deposition and background adsorption for this system ion deposition and subsequent TPD were done. The doses were done with the sample at 105 K and exposure to the ion beam for 30 min. Two experiments were carried out[1] and the results are plotted in Fig. 9, one for ''background adsorption,'' and one for D_2O^+ adsorption at 3 eV translational energy with D_2O pressure in the nozzle of about 2.5 Torr. The dosing conditions for the two experiments were identical except the sample bias. For the background check, the sample was biased at 410 V, higher than the ion energy of 393 eV. For the D_2O^+ dose, the sample was biased at 390 V. The sample current was 0 and 10.6 nA, respectively, which corresponds to a exposure of 0 and 0.08 ML. Shown are masses 20, 19, and 18. The background adsorption shows 0.004 monolayers of water species. The ion deposition gave 0.016 monolayers (gross) of adsorbed water. Surface hydrogen from an anomolously high background caused the isotopic exchange seen in Fig. 9. The net water adsorbed versus incident current (assuming all ions hitting surface stick or are neutralized) allowed us to calculate the ion sticking probability at this energy as about 1/7. The neutral background to *incident* ion dose is thus about 0.004 to 0.08, or 1:20. This implies a 20:1 ratio for ions to neutral dose, for a cryopumpable feed gas like D_2O.

E. Use example: Deposition of Cs^+ on hexane

This experiment in progress[7] gives some good examples of how to maximize the performance of the ion source. A 300 eV Cs^+ ion beam at about 2 nA is used to charge up thin films of hexane ices (5–125 monolayers) from 1 to 14 V, using 0.001–0.01 monolayers of Cs^+ ions. The dosing time needed is from 1 to 30 min. The ion beam is narrow in energy, but is only fair in its spatial uniformity at the target. Our computer controls the bias on the target, and monitors the current.

Typically, we commence with the ion beam shuttered off via the gate valve. After opening it, we immediately ramp the voltage on the target from about 3 V below the beam bias to 2 above it, to measure the ion stopping curve. The sample bias voltage is then set at about 299 V. When dosing an insulating film the ion current begins to decay over a few minutes (depending on its thickness), as the charge accumulates on the top of the film. We allow the ion current to decay to 1/3 or so of its initial value. The areas in the beam with less than the average ion fluence take longer to charge up, so they get more ion deposition time. The ion dose per unit area is now nearly constant over the sample, despite the nonuniform ion beam. We then take a quick stopping curve measurement (10 s at most). The beam energy is now set 1 V below the new stopping curve, and dosing continues again. The current decreases again as the sample charges. The cycle is repeated until a uniform charge is built up, to give a well-defined voltage change (which is confirmed by a later kelvin probe measurement of the work function change). The current has been recorded by the computer. The instantaneous current has significant capacitive offsets from the voltage ramps via stray capacitance. The numerical integral of that recorded current removes the capacitance effects, and accurately gives the charge deposited on the sample.

That the sample is uniformly charged is evident from the fact that even when the target hexane layer is charged up 10 V, the FWHM of the derivative of the stopping curve grows from 0.7 to only 0.9 V.

ACKNOWLEDGMENTS

The authors are very grateful for numerous discussions with Steve Barlow, Gary Leach, and Carl Lineberger on ion beam sources, Brian Maschhoff for design and construction, Kristine German for assembly, and John Price for computer software development. Funded by Chemical Sciences, Basic Energy Sciences Division, Department of Energy. Pacific Northwest National Laboratory is operated by Battelle Memorial Institute for the Department of Energy under Contract No. DE-AC06-76L0-1830. The Environmental Molecular Sciences Laboratory is a collaborative users' facility of the Office of Health and Environmental Research.

[1] H. Wang, J. P. Biesecker, M. J. Iedema, G. B. Ellison, and J. P. Cowin, Surf. Sci. **381**, 142 (1997).
[2] R. J. Speedy, P. G. Debenedetti, R. S. Smith, C. Huang, and B. D. Kay, J. Chem. Phys. **105**, 240 (1996); G. A. Kimmel and T. M. Orlando, Phys. Rev. Lett. **75**, 2606 (1995).
[3] T. L. Gilton, C. P. Dehnbostel, and J. P. Cowin, J. Chem. Phys. **91**, 1937 (1989); F. T. Wagner, in *Structure of Electrified Interfaces*, edited by J. Lipkowski and P. N. Ross (Wiley, New York, 1996), Chap. 9; E. M. Stuve, A. Krasnopolar, and D. E. Sauer, Surf. Sci. **335**, 177 (1995); I. Villegas and M. J. Weaver, J. Am. Chem. Soc. **118**, 458 (1996); for atmospheric water thin films see for example works of S. M. George (University of Colorado, Boulder) and J. T. Roberts (University of Minnesota).

[4] *Low-energy Ion Surface Interactions*, edited by J. W. Rabalais (Wiley, New York, 1994); D. Marton, *ibid.* pp. 486–93.
[5] H. Kang, S. R. Kasi, and J. W. Rabalais, J. Chem. Phys. **88**, 5882 (1988).
[6] N. Shamir, D. A. Baldwin, T. Darko, J. W. Rabalais, and P. Hochmann, J. Chem. Phys. **76**, 6417 (1982).
[7] A. A. Tsekouras, M. J. Iedema, and J. P. Cowin (unpublished).
[8] HeatWave (formerly Spectra-Mat) Inc. Watsonville, CA 95076.
[9] J. Vancura and Z. Herman, Chem. Phys. **151**, 249 (1991).
[10] J. H. Freeman, W. Temple, D. Beanland, and G. A. Gard, Nucl. Instrum. Methods **135**, 1 (1976); J. H. Freeman, D. J. Chivers, G. A. Gard, and W. Temple, *The Production of Heavy Ion Beams* (Chem. Div., AERE Harwell, Oxfordshire, 1977).
[11] Colutron Research Corp., Boulder, CO 80301.
[12] L. M. Branscomb, D. S. Burch, S. J. Smith, and S. Geltman, Phys. Rev. **111**, 504 (1958).
[13] *Atomic and Molecular Beam Methods*, Vol. 1, edited by G. Scoles (Oxford University, New York, 1988), especially Chap. 2 by D. R. Miller.
[14] A. S. Mullin, K. K. Murray, C. P. Schulz, and W. C. Lineberger, J. Phys. Chem. **97**, 10281 (1993), and private communications.
[15] A. Ando, Y. Takeiri, O. Kaneko, Y. Oka, K. Tsumori, E. Asano, T. Kawamoto, R. Akiyama, and T. Kuroda, Rev. Sci. Instrum. **66**, 5412 (1995); R. McAdams, R. F. King, and A. F. Newman, *ibid.* **61**, 2176 (1990).
[16] Very oddly, the source in Ref. 14 does not (I have inspected it first hand) have magnetic suppression of electrons. I can only speculate that a magnetized structural component or filament heater stray field is doing the job for them!
[17] *The Physics and Technology of Ion Sources*, edited by I. G. Brown (Wiley, New York, 1989).
[18] M. L. Vestal, C. R. Blakley, P. W. Ryan, and J. H. Futrell, Rev. Sci. Instrum. **47**, 15 (1976).
[19] D. R. Strongin, J. K. Mowlem, K. G. Lynn, and Y. Kong, Rev. Sci. Instrum. **63**, 175 (1992).
[20] Spectrum Solutions, P.O. Box 179, Russelton, PA 15076.
[21] McAllister Technical Services, W. 280 Prairie Ave., Coeur d'Alene, ID 83814.
[22] We had one (out of three) Cs^+ emitters which had up to 10 eV of energy width, which we suspect was due to high resistivity in a flawed source, and can be a problem in any of the the sources if it is run at too low a temperature.
[23] A. H. Bayati, D. Marton, S. S. Todorov, K. J. Boyd, J. W. Rabalais, D. G. Armour, J. S. Gordon, and G. Duller, Rev. Sci. Instrum. **65**, 2680 (1994).
[24] B. E. Winger, H.-J. Laue, S. R. Horning, R. K. Julian, Jr., S. A. Lammert, D. E. Riederer, Jr., and R. G. Cooks, Rev. Sci. Instrum. **63**, 5613 (1992); V. Franchetti, B. H. Solka, W. E. Baitinger, J. W. Amy, and R. G. Cooks, Int. J. Mass Spectrom. Ion Processes **23**, 29 (1977), and to be published.